MATHEMATICAL DESCRIPTION OF A BURSTING PACEMAKER NEURON BY A MODIFICATION OF THE HODGKIN-HUXLEY EQUATIONS

R. E. PLANT *and* M. KIM

From the Department of Mathematics, University of California, Davis, California 95616, and the School of Electrical Engineering, Cornell University, Ithaca, New York 14853

ABSTRACT Modifications based on experimental results reported in the literature are made to the Hodgkin-Huxley equations to describe the electrophysiological behavior of the *Aplysia* abdominal ganglion R15 cell. The system is then further modified to describe the effects with the application of the drug tetrodotoxin (TTX) to the cells' bathing medium. Methods of the qualitative theory of differential equations are used to determine the conditions necessary for such a system of equations to have an oscillatory solution. A model satisfying these conditions is shown to predict many experimental observations of R15 cell behavior. Numerical solutions are obtained for differential equations satisfying the conditions of the model. These solutions are shown to have a form similar to that of the bursting which is characteristic of this cell, and to predict many results of experiments conducted on this cell. The physiological implications of the model are discussed.

INTRODUCTION

The central nervous systems of invertebrates contain many cells which display a regular spontaneous activity in the absence of any synaptic input. This activity generally occurs in one of two modes: regular firing (known as "beating"), or clusters of spikes separated by long periods of hyperpolarization (known as "bursting") (Carpenter, 1973). The abdominal ganglion of the mollusc *Aplysia* contains cells which display both of these behaviors (Frazier et al., 1967); in particular, the cell designated R15 by Frazier et al. normally fires in the bursting mode.

There is strong evidence (Carpenter, 1973, Junge and Stephens, 1973) that the bursting of cell R15 is due to a cyclic variation in potassium conductance. Strumwasser (1968) found that application of the drug tetrodotoxin (TTX) to the cells' bathing medium resulted in the abolition of action potentials and the emergence of an underlying slow oscillation. Mathieu and Roberge (1971) reported the effects of experimental injection of currents through the membrane of the TTX-treated cell. However, the mechanism which causes the cyclic variation in potassium conductance underlying the slow wave has not been determined. In a previous paper (Plant and Kim, 1975) a qualitative method was developed to determine a model based on experimental results in the

literature, which would predict the experimental observations of the slow wave. In this paper, we use this method to modify the Hodgkin-Huxley equations (Hodgkin and Huxley, 1952) through the addition of terms, the existence of which may be inferred from published experimental results, to describe the behavior of an R15 cell bathed in a medium containing TTX. Qualitative conditions are then determined which are sufficient for a two-dimensional approximation of the model to have a limit cycle. A numerical example of the model is then given. The solutions of this example are shown to display bursting and to duplicate many, but not all, experimental results. The physiological implications of the model are then discussed, and a more complicated version of the model is presented which predicts recent results not predicted by the simpler model.

LIST OF SYMBOLS

V	Membrane voltage
C	Membrane capacitance
V_I	Nernst equilibrium potential of combined inwardly flowing ions
V_K	Nernst equilibrium potential of K^+ ions
V_L	Nernst equilibrium potential of leakage ions
X_i	"Activation" term
Y_i	"Inactivation" term
$\tau_{Xi}(V)$	"Activation" time constant
$\tau_{Yi}(V)$	"Inactivation" time constant
$S_i(V)$	Steady-state "activation"
$Z_i(V)$	Steady-state "inactivation"

($i = I, K, A, P$)

g_i	Maximum ionic conductance, $i = I, K, A, P, L$
g_T	Inward conductance in the presence of TTX
I_{ep}	Ionic electrogenic pump current
I_{ext}	External current controlled by the experimenter
t	Time

The subscripts I, K, A, P, T, L correspond to membrane channels. In Hodgkin and Huxley's (1952) notation, τ_m corresponds to τ_{XI}, m_∞ to $S_I(V)$, etc.

The functions $S_i(V)$ and $Z_i(V)$ are defined as having the following properties (see Fig. 1).

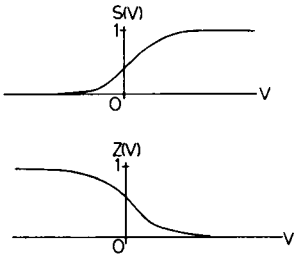

FIGURE 1 Typical S and Z functions as described in the text.

$$
\begin{array}{lll}
 & S_i(V) & Z_i(V) \\
\text{(a)} & \lim_{V \to +\infty} S_i(V) = 1 & \lim_{V \to +\infty} Z_i(V) = 0 \\
 & \lim_{V \to -\infty} S_i(V) = 0 & \lim_{V \to -\infty} Z_i(V) = 1 \\
\text{(b)} & dS_i/dV \geq 0 & dZ_i/dV \leq 0.
\end{array}
$$

ANALYSIS OF THE PROBLEM

In our notation, the Hodgkin-Huxley equations are:

$$\dot{V} = (1/C)[g_l X_l^3 Y_l (V_l - V) + g_K X_K^4 (V_K - V) + g_L (V_L - V) + I_{ext}], \quad (1\,A)$$

$$\dot{X}_I = [1/\tau_{XI}(V)][S_I(V) - X_I],$$

$$\dot{Y}_I = [1/\tau_{YI}(V)][Z_I(V) - Y_I], \quad (1\,B)$$

$$\dot{X}_K = [1/\tau_{XK}(V)][S_K(V) - X_K].$$

These equations were formulated to describe the behavior of the squid giant axon (Hodgkin and Huxley, 1952). In a voltage clamp experiment, when the membrane potential is changed from near its resting value to a more depolarized level, the potassium current in this axon is observed to asymptotically approach a new value in a monotonically increasing manner. When a similar experiment is performed on the R15 cell, the potassium current is observed to increase rapidly to a peak, and then decrease monotonically to its new value (Faber and Klee, 1972). A similar phenomena was analyzed in nudibranch central neurons by Connor and Stevens (1971), who found that this current sag could be explained by invoking a second potassium channel, here denoted by the subscript A, independent from the Hodgkin-Huxley K channel, which contained an inactivation as well as an activation term. Mathematically, Eq. 1 A of the Hodgkin-Huxley equations may be replaced by

$$\dot{V} = (1/C)[g_l X_l^3 Y_l (V_l - V) + (g_K X_K^4 + g_A X_A Y_A)(V_K - V) + g_L (V_L - V) + I_{ext}], \quad (2)$$

and the corresponding activation and inactivation terms are added to the system, namely,

$$\dot{X}_A = [1/\tau_{XA}(V)][S_A(V) - X_A],$$

$$\dot{Y}_A = [1/\tau_{YA}(V)][Z_A(V) - Y_A]. \quad (3)$$

There are three differences between Eq. 2 and the corresponding equation of Connor and Stevens: in the Connor-Stevens equation there are two potassium K activation terms, the equilibrium potential of the A system is slightly different from V_K, and X_A is raised to the fourth power. None of these differences will affect the qualitative behavior of Eq. 2.

Connor and Stevens also reported, but did not include in their equation, a third potassium "channel," having an activation time constant much longer than any of the others observed in the system. What may be a similar phenomenon was observed by Junge and Brodwick (1970) in the *Aplysia* R2 cell, and its existence in R15 may be inferred from Junge and Stephens' (1973) measurements of a very slow potassium conductance change. In addition, *Aplysia* cells are known to contain an electrogenic sodium pump (Cooke et al., 1974) generating a hyperpolarizing current, which will be assumed constant. The effect of these terms will be to replace Eq. 2 by

$$\dot{V} = (1/C)[g_I X_I^3 Y_I(V_I - V) + (g_K X_K^4 + g_A X_A Y_A + g_P X_P)(V_K - V) + g_L(V_L - V) + I_{ep} + I_{ext}] \quad (4)$$

with the addition of the equation

$$\dot{X}_P = (1/\tau_{XP})[S_P(V) - X_P]. \quad (5)$$

We shall assume that τ_{XP} is not a function of voltage, and that

$$\tau_{XI}(V), \tau_{YI}(V), \tau_{XK}(V), \tau_{XA}(V), \tau_{YA}(V) \ll \tau_{XP},$$

for all values of V. We will assume that when the cell is bathed in a medium containing TTX, the variability of the I channel is eliminated (Narahashi et al., 1964; Sastre, 1974). Recent experimental results (Smith et al., 1975) indicates that bursting cells possess an inward channel (possibly Na^+-conducting) which does not inactivate completely. The simplest (in terms of economy of variables) modification of the equations consistent with such results is the addition of a constant term, g_T. (The consequences of a more complicated model, with voltage-dependent behavior in a second channel, is examined in the Discussion). We will add this term, and further assume that its value is not affected by the addition of TTX to the bathing medium. Our final system of equations for the R15 cell in a normal medium is then

$$\dot{V} = (1/C)[(g_I X_I^3 Y_I + g_T)(V_I - V) + (g_K X_K^4 + g_A X_A Y_A + g_P X_P)(V_K - V) + g_L(V_L - V) + I_{ep} + I_{ext}], \quad (6)$$

together with Eqs. 1 B, 3, and 5. In a medium containing TTX, assume $g_I = 0$ and we get

$$\dot{V} = (1/C)[g_T(V_I - V) + (g_K X_K^4 + g_A X_A Y_A + g_P X_P)(V_K - V) + g_L(V_L - V) + I_{ep} + I_{ext}] \quad (7)$$

instead of Eq. 6. We propose Eqs. 1 B, 3, 5, 7 as a model for the behavior of the R15 cell, with Eqs. 1 B, 3, 5, 7 as a model for its behavior in TTX. In the Appendix we demonstrate that for certain values of the components of the model, we may expect Eqs. 1 B, 3, 5, 7 to have an oscillatory solution, and in the Discussion we demonstrate that this solution may be predicted to simulate the behavior of R15 in TTX. In the

next section we demonstrate numerically that a properly chosen example of the model has a bursting solution.

DEVELOPMENT OF A NUMERICAL EXAMPLE

We start with the basic Hodgkin-Huxley equations, modified to make depolarization of the membrane positive, in accord with recent notation (Fitzhugh, 1969, p. 24). First these will be modified to account for the observation that the conductance of the R15 membrane is approximately $\frac{1}{100}$ that of the squid giant axon (Carpenter, 1973). Thus, we divide all of the conductances by one hundred. The values of V_{Na} and V_K in the Hodgkin-Huxley model were set so as to make the resting potential equal to zero; we will use the values of V_{Na} and V_K given in the literature for the R15 cell. Thus, we must rescale the voltage in the equations for the time constants and steady-state terms in Eqs. 1 B, 3, 5, and 7 in the following way:

$$V_{R15} = a\,V_{squid} + b, \tag{8}$$

where

$$a = (V_{Na} - V_K)_{squid}/(V_I - V_K)_{R15},$$

$$b = [(V_{Na})_{squid}(V_K)_{R15} - (V_I)_{R15}(V_K)_{squid}]/(V_K - V_I)_{R15}.$$

Better results are obtained by further translations of V_{R15} (i.e. other than the addition of the factor b); these are incorporated in the development.

Finally, to account for the observation (Carpenter, 1973) that the R15 membrane is relatively more permeable to sodium and less to potassium than the squid membrane we raise the value of the term g_I from 1.2 to 4. Following Wachtel and Wilson (1973) we set V_I at 30 mV and V_K at −75 mV. We let V_L equal −40 mV. The time

TABLE I

PARAMETERS AND FUNCTIONS OF THE MODEL RESULTING FROM MODIFICATION OF THE HODGKIN-HUXLEY EQUATIONS

$g_I = 4.0$	$g_K = 0.30$	$g_L = 0.003$ (mho $\times 10^{-3}$)
$V_I = 30$	$V_K = -75$	$V_L = -40$ (mV)
$C = 1\,\mu F$		
$S_I(V) = \alpha_m/(\alpha_m + \beta_m)$	$Z_I(V) = \alpha_h/(\alpha_h + \beta_h)$	$S_K(V) = \alpha_n/(\alpha_n + \beta_n)$
$\tau_{XI} = 12.5/(\alpha_m + \beta_m)$	$\tau_{YI} = 12.5/(\alpha_h + \beta_h)$	$\tau_{XK} = 12.5/(\alpha_n + \beta_n)$

where

$$\alpha_m(V) = \frac{0.1[-26 - 1.2V]}{\exp([26 - V]/10) - 1} \qquad \beta_m(V) = 4\exp([51 - 1.2V]/18)$$

$$\alpha_h(V) = 0.07\,\frac{\exp(-51 - 1.21V)}{20} \qquad \beta_h(V) = \frac{1}{\exp([21 - 1.3V]/10) + 1}$$

$$\alpha_n(V) = \frac{0.01[-21 - 1.21V]}{\exp([-21 - 1.21V]/10) - 1} \qquad \beta_n(V) = 0.125\exp([-31 - V]/80)$$

TABLE II

PARAMETERS ADDED TO THE MODIFIED HODGKIN-HUXLEY EQUATIONS TO SIMULATE THE R15 CELL

$g_T = 0.008$ $\quad g_A = 0.06$	$g_P = 0.015$ $\quad$ (mho $\times 10^{-3}$)
$S_A(V) = [1 + \exp(-0.08[V + 45])]^{-1}$	$Z_A(V) = [1 + \exp(0.27[V + 50])]^{-1}$
$\tau_{XA} = 10$ ms	$\tau_{YA} = 235$ ms
$S_P(V) = [1 + \exp(-0.7[V + 47])]^{-1}$	$I_{ep} = -0.22\ \mu$A
$\tau_{XP} = 8{,}000$ ms	

constants of the modified Hodgkin-Huxley parameters are obtained by comparison of the spike widths of the R15 and squid giant axon. The squid axon has a spike width of approximately 2 ms, while that of the R15 cell is approximately 25 ms, so that the Hodgkin-Huxley time constants are multiplied by 12.5. The parameters of our Eqs. 1 B, 3, 5, and 6 which result from modification of the Hodgkin-Huxley equations are given in Table I. The value $C = 1\ \mu$F has been chosen to match that of Hodgkin and Huxley. The model is therefore based on a membrane patch having a capacitance of 1 μF, rather than an area of 1 cm^2. We now must choose the additional parameters of the system in such a way as to satisfy the conditions derived in the Appendix such that the reduced system, Eqs. 12, has a limit cycle. In keeping with the formulations of Hodgkin and Huxley, we will use exponential logistic functions to describe our S and Z functions. These are functions of the form

$$f(V) = [1 + \exp(-\gamma[V - \theta])]^{-1},$$

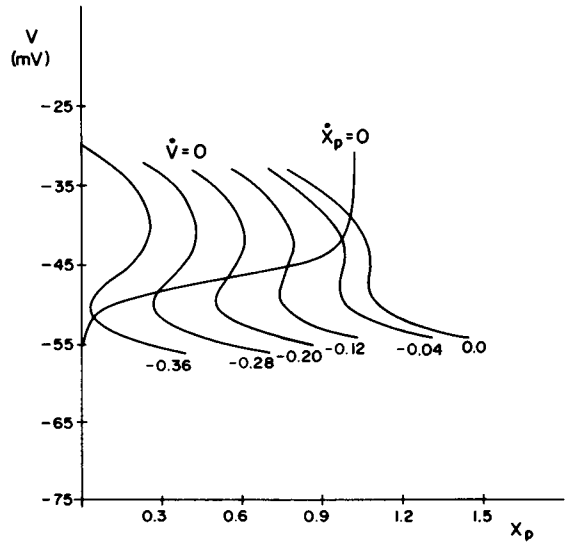

FIGURE 2 Phase portrait of the nullclines of system 12 for several values of the parameter ($I_{ext} + I_{ep}$); these values are shown beneath each $\dot{V} = 0$ nullcline.

where $|\gamma|$ is the maximum magnitude of the slope of f, occurring at the inflection point, and θ is the location on the V axis of the inflection point. It was found that multiplication of the Hodgkin-Huxley time constants by a factor of 12.5 brought them within the range of the corresponding time constants of Connor and Stevens. For this reason, Connor and Stevens' values for the A-channel time constants were used in our model. The additional parameters are listed in Table II. For purposes of comparison, the Connor and Stevens data for their Z_A term may be represented by $Z_{ACS} = [1 + \exp(0.04[V + 70])]^{-1}$. The reason for this difference will be considered in the Discussion.

Fig. 2 shows the nullclines of $\dot{V} = 0$ and $\dot{X}_p = 0$ of the two-dimensional system 12 drawn in the (V, X_P) phase plane. It is evident that for values of $I_{ep} + I_{ext}$ between approximately -0.05 and -0.30 the nullclines will intersect in a region of positive slope of the $\dot{V} = 0$ nullclines. Thus our analysis predicts that the system of equations 12 with parameters given in Tables I and II will have a stable limit cycle, and that for large values of τ_{XP} the system of equations 1 B, 3, 5, and 7 will have a periodic, oscillatory solution. In the next section we analyze the full model numerically.

NUMERICAL ANALYSIS

In this section we analyze the example of our model developed in the last section, and perform numerical "experiments" with it. It is shown that the model of the system in TTX displays an oscillatory solution. This system being itself a special case of the full system in which the variable terms involving inward current are abolished, we then restore these terms to the system to demonstrate that the full system displays the properties of bursting. When reference is made in this section to the equation the parameters will be assumed to have the values developed in the last section.

Two classes of methods for the numerical solution of ordinary differential equations are commonly used: the single step (e.g., Runge-Kutta) method and the multistep (e.g., Adams-Moulton) method (Hamming, 1973). A comparison was first made between these two methods to determine which was best suited for this problem. Programs were written to solve the equations using each method. The variable step size Adams-Moulton method was found to have extremely severe "step size oscillation" problems (Hamming, 1973, p. 410) and was rejected. The slightly increased speed of the fixed step size Adams-Moulton method was offset by the greater accuracy of the Runge-Kutta method, and the latter was selected as the method of choice for the problem. For a more detailed comparison of these methods as applied to the solution of the Hodgkin-Huxley equations see Moore and Ramon (1974).

In the initial computer runs, an approximate method was used in which, when the system was varying slowly, the fastest variables were set to their steady-state values and the step size was increased accordingly (Noble, 1962). In the runs whose results are displayed in this paper, this approximation was abandoned and the full system was always used. The step size was successively halved until further reduction did not change the solution significantly (for $t \leq 1$ s, $|V_h - V_{h/2}| < 0.1$). The final step size

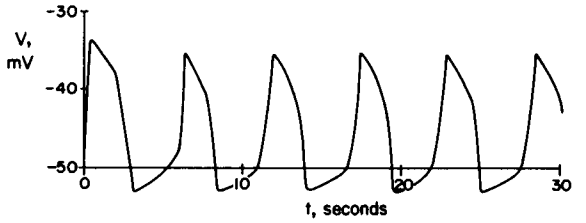

FIGURE 3 Numerical solution of Eqs. 12 for $I_{ext} = 0$.

used was 1 ms. The programs were written in FORTRAN, and run on Cornell University's IBM 370/168 computer after being compiled in FORTRAN H. No run took longer than 2 min CPU time.

The first numerical "experiment" is to verify that Eqs. 12 actually have a stable limit cycle. Fig. 3 shows the solution of Eqs. 12 for $I_{ext} = 0$ and confirms a periodic, oscillatory solution. The next test is to return to the full system of equations 1 B, 3, 5, and 7. Fig. 4 shows the solution of these equations for three values of I_{ext}. The system 1 B, 3, 5, and 7 is seen to move more slowly than the system 12, which is due to the fact that three of the differential equations of the full system have been replaced by algebraic equations in the reduced system. Table III gives the period and amplitude of the slow wave for three valves of I_{ext}. Both the period and amplitude are seen to decrease with depolarizing current and increase with hyperpolarizing current, as predicted in the Discussion from geometrical considerations. The slow wave is thus seen to conform to all the experimental observations of Mathieu and Roberge (1971). Following this confirmation, Eq. 6 was substituted for Eq. 7 in the model to test whether the full system would display bursting as seen in the R15 cell. Fig. 5 gives the results of this computer run for three values of $I_{ext} + I_{ep}$. For $I_{ext} = 0$ (Fig. 5 *a*), the system is seen to display bursting of a form very similar to that of the R15 cell. The reason for the lack of low frequency leading spikes in the burst will be given in the Discussion. For $I_{ext} + I_{ep} = 0$ (or $I_{ext} = +0.22$), Fig. 5 *b*, top trace, the system is seen to display "beating," due to the slow wave's state point being fixed at a stable upper equilibrium point.

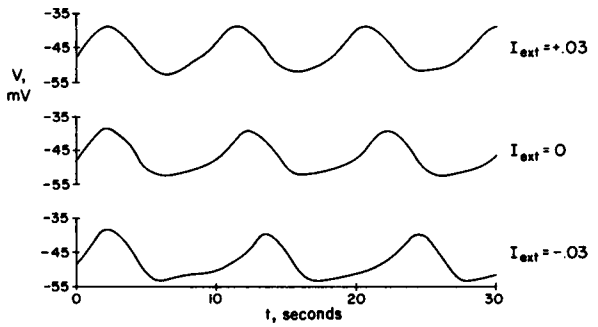

FIGURE 4 Numerical solution of Eqs. 1 B, 3, 5, 7 for three values of I_{ext}, shown to the right of the plots.

TABLE III

PERIOD AND AMPLITUDE OF OSCILLATIONS OF SYSTEM 1 B, 3, 5, 7, WITH PARAMETERS AS IN TABLES I, II, AND III

I_{ext}	Period	Amplitude
μA	s	mV
+0.03	9.3	12.6
0	9.9	13.3
−0.03	10.9	13.5

We have observed that the R15 cell occasionally spontaneously alters its output from a bursting to a beating mode. When the cell is in the beating mode, the injection of hyperpolarizing current through the recording electrode will return the cell to a bursting mode. Upon cessation of the current injection the cell returns to a beating mode. Fig. 6 shows the results of one such experiment. By the application of ouabain, Junge and Stephens (1973) have demonstrated that the beating mode of the R15 cell is associated with the abolishment of the electrogenic pump current. For $I_{ext} = -0.14$, Fig. 5 *b*, bottom trace, the spontaneous activity is abolished, due to the slow wave's state point being moved to a lower stable equilibrium point. Thus the model is seen to adequately predict the result of experiments.

Eaton (1972) has argued that the current "sag" displayed in voltage clamping experiments is due not primarily to potassium inactivation, but to potassium accumulation. This argument is based on results (Eaton, 1972, Table 2) which show that for step changes in voltage from −40 mV to −2 mV, the ratio of peak to final conductance does

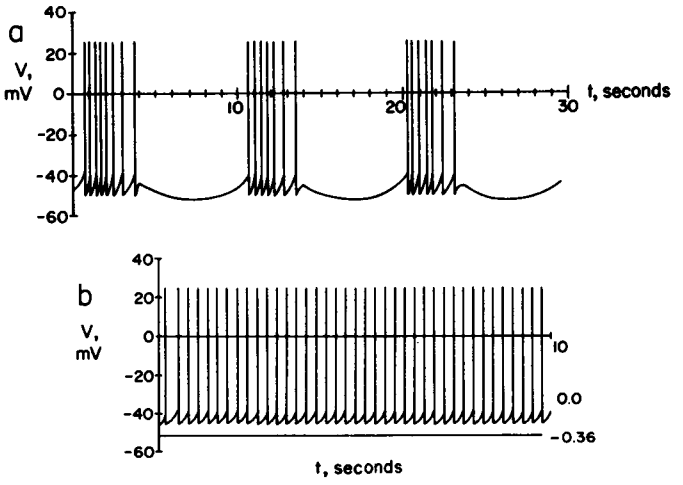

FIGURE 5 Numerical solution of Eqs. 1 B, 3, 5, 6. (*a*) $I_{ext} = 0$; solution displays bursting. (*b*) Upper plot: $I_{ext} = +0.22(I_{ext} + I_{ep} = 0)$; solution displays beating. Lower plot: $I_{ext} = -0.14$ $(I_{ext} + I_{ep} = -0.36)$; oscillation is abolished.

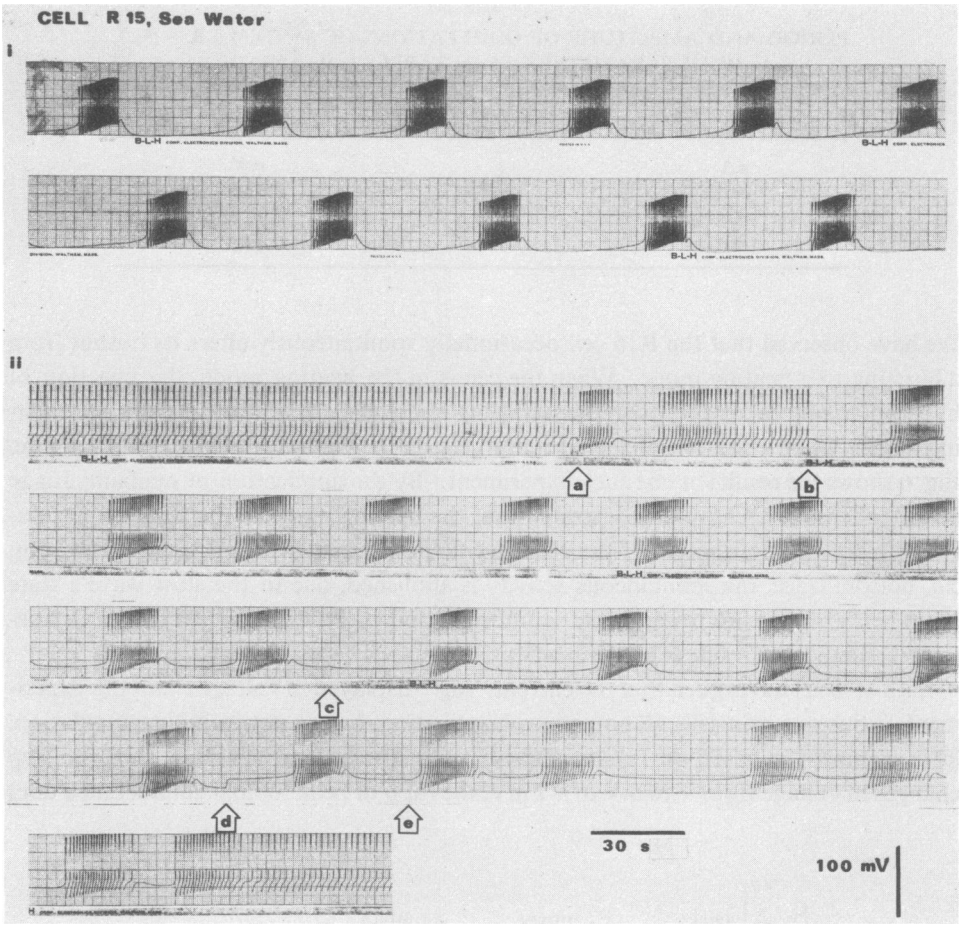

FIGURE 6 Results of experiments with R15 cell. (I) Normal bursting model. (II) Recorded later, showing cell in beating mode. At arrow *a* hyperpolarizing current is injected. At arrow *c*, hyperpolarizing current injection ceased. Arrows *b*, *d*, and *e* represent artifacts.

not drop more than 30%. This result is in accord with our model since at -40 mV, our potassium inactivation parameter has a steady state value $Z_A(-40) = 0.063$. We would thus argue that current sag in step changes from -40 mV to -2 mV is indeed due to potassium accumulation since the potassium inactivation "channel" is almost completely inactivated, but that in step changes from a more hyperpolarized state, potassium inactivation should also be observed (Fig. 7). Fig. 8 shows the steady-state current voltage relationship (solid line) of system 1 *b*, 3, 5, 6. The dashed lines in Fig. 8 represent typical *I-V* curves for (*a*) an ordinary nerve cell, and (*b*) for a cell displaying anomalous rectification (Faber and Klee, 1972). The negative slope steady-state conductance may be regarded as a more "advanced" form of anomalous rectification. This *I-V* curve is in good agreement with experimental results (Gola, 1974;

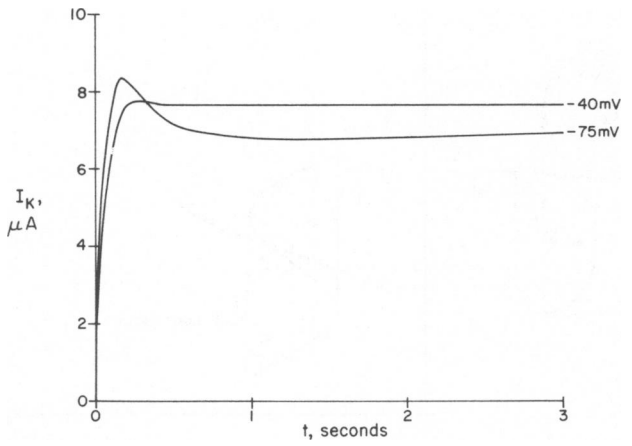

FIGURE 7

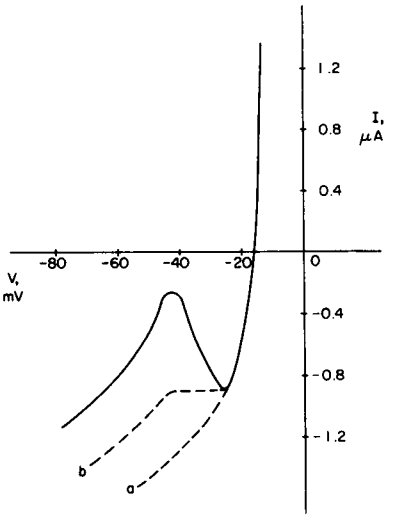

FIGURE 8

FIGURE 7 Numerical solution of potassium current under voltage clamp conditions. Solution is for $V = -2$ mV starting from initial values of V as shown.

FIGURE 8 Steady-state I-V relationship of the model. Dashed line *a* shows the typical I-V curve of a normal nerve cell, dashed line *b* shows that of a cell displaying anomalous rectification.

Smith et al., 1975; Wilson and Wachtel, 1974). It must be emphasized that the I-V curve is *not* a phase plane nullcline, and should not be confused with "N" or "S" shaped curves such as those of Fig. 2.

DISCUSSION

In an earlier paper (Plant and Kim, 1975), the two-dimensional model developed in the Appendix was used to predict qualitatively and suggest an interpretation of many experimentally observed behaviors of the *Aplysia* R15 cell in TTX. We will discuss these in greater detail here. First, we give a descriptive account of the events of one cycle of the slow wave. Starting at $t = 0$ (Fig. 4), the term $g_A S_A Z_A$ has a low value, and the term g_T of Smith et al. causes V to rise toward V_I. This rise is arrested and turned around by the activation of the term X_P. The drop toward V_K is then accelerated by the regenerative effect of the inactivation Y_A. The effect of this inactivation is then abolished by the dropping in value of X_A, and the cycle repeats. As observed by Mathieu and Roberge (1971), the amplitude and period of the slow wave are both increased by passing a hyperpolarizing current through the membrane, and decreased by a depolarizing current. The geometrical interpretation of this phenomenon is given in Fig. 9. Referring to this figure, the structure of the equation $X_P = G(V)$ (Eq. 13) makes the one parameter family of curves dependent on I_{ext} fold under themselves as I_{ext} becomes more negative (this can also be seen in Fig. 2). Thus the dimension a_l, which is the amplitude of the discontinuous oscillation, becomes larger as I_{ext}

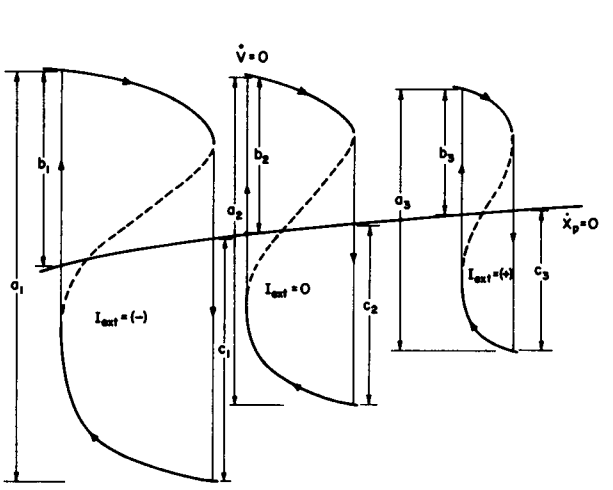

FIGURE 9

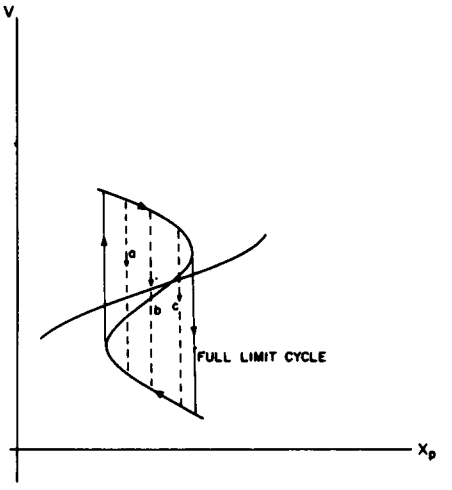

FIGURE 10

FIGURE 9 Qualitative behavior of the system 12 for hyperpolarizing, zero, and depolarizing external current. See text for further explanation.

FIGURE 10 Explanation of the phenomenon of "resetting." Dashed lines a, b, c, represent the effects of strong hyperpolarizing currents applied at successively later points in a burst. Thin line represents full limit cycle.

becomes less positive or more negative. Furthermore, as the state point jumps from one stable portion of the curve (shown as the heavy lines of Fig. 9) to another, the amount of time that it spends on a given portion is an increasing function of that portion's distance from the slow (X_p) nullcline. These distances, shown as b_i and c_i in Fig. 9 are seen to increase as I_{ext} becomes more negative, with the c_i increasing more than the b_i.

When a stronger depolarizing or hyperpolarizing current is passed through the membrane, the membrane oscillation is seen to stop, leaving the voltage at a fixed point near the maximum or minimum value of the potential when it was oscillating (Mathieu and Roberge, 1971). Referring to Fig. 2, with $I_{ep} = -0.22$, it can be seen that sufficiently large positive or negative values of I_{ext} will move the $\dot{V} = 0$ nullcline to a position where it intersects the $X_p = 0$ nullcline at a stable equilibrium point, and that the stable point is near the maximum or minimum value of the oscillation. The model also predicts the effect of ouabain, which is to abolish the membrane oscillation at a point near the maximum oscillatory value (Junge and Stevens, 1973); Junge and Stevens also showed that the application of a hyperpolarizing current would restart the oscillation. In the model, with $I_{ext} = 0$, the effect of ouabain would be to make I_{ep} equal zero, moving the equilibrium point to a stable position (Fig. 2). Setting I_{ext} equal to a negative value returns the system to an oscillatory mode. Strumwasser (1973) has observed that the addition of Li^+ abolishes the slow wave. This may be explained in terms of our model by assuming that Li^+ makes the T component ineffective.

Finally, we examine the phenomenon of resetting (Strumwasser, 1967). When a hyperpolarizing current strong enough to artificially terminate a burst is passed through the membrane, and then the external current is returned to zero, the bursting process is "reset" in phase (Winfree, 1970). The phase relationship between the reset cycle and the original cycle depends on the position in the burst at which the hyperpolarizing current was applied. If the hyperpolarizing current was applied early in the burst, the reset burst occurs almost immediately after termination of hyperpolarization. As the current is applied later in the burst, the length of time between termination of the current and the onset of the reset burst increases. The mechanism of this phenomenon is explained graphically in Fig. 10. Dashed lines *a*, *b*, and *c* represent the effects of a strong hyperpolarizing pulse applied at successively later points in the burst. In each case the state point is moved off the upper portion onto the lower portion (the interburst hyperpolarization), due to an instantaneous rightward shift of the $V = 0$ nullcline (Fig. 2), but the time required to reattain the upper portion is successively increased.

It is evident that other dynamic terms could be used in place of those in Eq. 6, and still result in a limit cycle in system 12. For instance, consider a slow sodium inactivation in place of X_P. If X_P is replaced by an inactivation term Y_Q with a large time constant, Eq. 6 becomes

$$\dot{V} = (1/C)[(g_I X_I^3 Y_I + g_Q Y_Q + g_T)(V_I - V) + (g_K X_K^4 + g_A X_A Y_A)(V_K - V) + g_L(V_L - V) + I_{ep} + I_{ext}], \quad (9)$$

and it is easy to show that a reduced system similar to that of Eqs. 12 may have a limit cycle. However, unlike both Eqs. 12 and the real R15 cell, a reduced system based on Eq. 9 has a limit cycle which decreases in amplitude with increasing hyperpolarizing current, and thus Eq. 9 must be regarded as being less likely than Eq. 6. Lux and Eckert (1974) report the existence of a "slow" inward current. While this current is indeed slow, its time constant is still an order of magnitude less than τ_{XP}, and thus, in terms of our model, the current is "relatively fast." Their results may be interpreted as supporting the two variable inward channel model discussed in the second to last paragraph of this paper.

There are three differences in the waveshapes of the burst between our model and the typically observed output of the *Aplysia* R15 cell: (*1*) There are no low frequency leading spikes in the burst; (*2*) the spike undershoot in the model remains constant rather than decreasing; (*3*) the spike width in the model remains constant throughout the burst. In the R15 cell, the spike width increases during the burst (Strumwasser, 1967). We shall consider each of these differences in turn.

The absence of leading spikes in the burst may be explained as follows. It was originally postulated that the relaxation time of the voltage process was much less than that of the X_P process. This results in almost discontinuous motions in the phase space (Fig. 11, solid line). Numerical experiments indicate that a similar time course could have been obtained by increasing the relaxation time of the V equation and

decreasing that of the X_P equation. This would have given a smooth oscillation (Fig. 11, dashed line) which would have resulted in the appearance of leading spikes.

The constant post spike hyperpolarizing undershoot is probably due to the lack of potassium accumulation effect in the model. The effect of potassium accumulation is to raise this undershoot during multiple spiking, (Frankenhaeuser and Hodgkin, 1956). However, based on the results of Eaton (1972, Fig. 2), such an effect cannot be ascribed to a simple one dimensional process such as that postulated for the squid axon by Frankenhaeuser and Hodgkin, since the equation describing such a process, although nonlinear, would have a generally exponential type solution, while the time course of the process underlying Eaton's results is evidently sigmoidal.

The membrane phenomena underlying the increase in spike width are more difficult to explain. Increased spike width due to the application of TEA has been associated with an increase in the potassium activation time constant τ_{YK} (Fitzhugh, 1969). However, not enough is yet known to discuss this matter further.

Other than variations in waveshape, there are two main discrepancies between our model and experimental observations. The first is that our function $Z_A(V)$ has a maximum slope of magnitude 0.27, while the function $S_A(V)$ has a maximum slope of 0.08 (see Table II). Experimental results (e.g., Connor and Stevens, 1971) indicate that the functions S_A and Z_A should have maximum slopes which are similar in magnitude. The second is that recent evidence (Smith et al., 1975) indicates that the regenerative mechanism responsible for membrane oscillations is at least partially active in the absence of internal potassium.

Both of these discrepancies may be accounted for by the assumption of a second inward current term (Lux and Eckert, 1974). We will call this term g_C and we will assume that it contains an activation term whose time constant is of the same order as τ_{YA}. In terms of our model, this would imply that Eq. 6 should be replaced by

$$\dot{V} = (1/C)[(g_I X_I^3 Y_I + g_T + g_C X_C)(V_I - V) + (g_K X_K^4 + g_A X_A Y_A + g_P X_P) \cdot (V_K - V) + g_L(V_L - V) + I_{ep} + I_{ext}], \quad (10)$$

together with the supplementary equation

$$\dot{X}_c = [1/\tau_{XC}(V)][S_C(V) - X_C]. \quad (11)$$

An analysis of the model 1 B, 3, 5, 10, 11, identical with that of the Appendix shows that condition I is replaced by I':

$$\frac{g_C S_C'(V_I - V)}{(V - V_K)} + |g_A S_A Z_A'| > + g_K(S_K^4)' + g_A S_A' Z_A + \frac{(g_T + g_C S_C)(V_I - V_K) + g_L(V_K - V_L) + (I_{ep} + I_{ext})}{(V - V_K)^2}. \quad (I')$$

The physiological significance of replacing condition I with I' is evident. With $g_C = 0$ as in Eq. 6, the potassium activation is required to provide all the regenerative effect

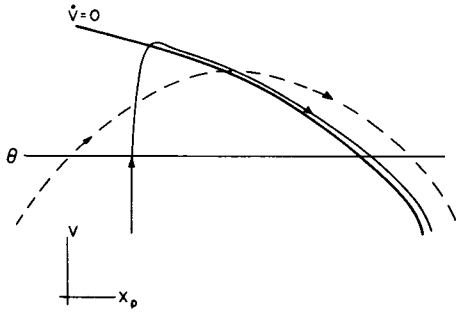

FIGURE 11

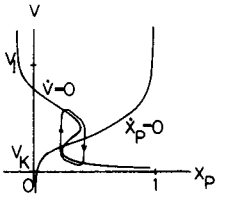

FIGURE 12

FIGURE 11 Phase plane explanation of the lack of leading spikes in the model's bursts. Heavy line denotes $\dot{V} = 0$ nullcline. Solid line, phase trajectory as in model. Dashed line, as presumed to exist in the real cell. θ denotes the cell threshold level.

FIGURE 12 Phase plane of the system 12 showing graphically the conditions required for a limit cycle.

of the slow wave, and hence must have a slope with a large magnitude. If Eq. 6 is replaced by 10, 11, then the function $S_C(V)$ augments the regenerative effect of $Z_A(V)$. This would permit $Z_A(V)$ to have a slope with a smaller magnitude, and would provide a regenerative effect in the absence of internal potassium.

The values of certain parameters of our model are not available from experimental data at this time. It is hoped that this model will provide an impetus for experimenters to attempt to measure these parameters, either directly or indirectly. Our work shows that a model consisting of Eqs. 1 B, 3, 5, 6, with properly chosen parameters simulates the behavior of the R15 cell. A model consisting of Eqs. 1 B, 3, 5, 10, 11, is shown to predict experimental results not predicted by the simpler model. In addition to these specific results, there are two results of a more general nature. The first is that activation and inactivation may exchange their respective roles of regeneration and degeneration in Hodgkin-Huxley type models, and the second is that these models may couple periodic voltage oscillations of different relative frequencies to produce oscillations with complex waveshapes.

R. E. Plant would like to thank Dr. J. C. Dunn for many helpful discussions of the problem, and Doctors L. Payne and S. Levin for obtaining partial support for this work under National Science Foundation Grant GP-33031X. This work was also supported in part by NSF Grant GB-35498.

Received for publication 16 January 1975 and in revised form 7 April 1975.

APPENDIX

In this section we review the arguments presented in an earlier paper (Plant and Kim, 1975). The problem is to find conditions which are sufficient for the system represented by Eqs. 1 B, 3, 5, 7, to have a periodic, oscillatory solution. Since this is a five-dimensional nonlinear system, this problem cannot be solved directly. Rather, we must try to approximate system 1 B, 3, 5, 7

by a two-dimensional system so that we may use the phase plane techniques of Poincafe to analyze this approximate system.

In order to form an approximate system, we note that the variables $\dot{X}_K$, $\dot{X}_A$, and $\dot{Y}_A$ have time constants much less than that of $\dot{X}_P$. We may therefore approximate system 1 B, 3, 5, 7 by multiplying the left-hand sides of the differential equations for $\dot{X}_K$, $\dot{X}_A$, and $\dot{Y}_A$ by a parameter ϵ, and letting ϵ go to zero. We then make use of a theorem of Tikhonov (Tikhonov, 1950; Plant and Kim, 1975) which states that if a certain function, which we call the Tikhonov function, is negative definite then the solution of the system 1 B, 3, 5, 7 will approach that of the system

$$\begin{aligned} \dot{V} &= (1/C)[g_T(V_I - V) + [g_K S_K^4(V) + g_A S_A(V) Z_A(V) + g_P X_P](V_K - V) \\ &\quad + g_L(V_L - V) + I_{ep} + I_{ext}], \\ \dot{X}_P &= (1/\tau_{XP})[S_P(V) - X_P], \\ X_K &= S_K(V), X_A = S_A(V), Y_A = Z_A(V), \end{aligned} \tag{12}$$

in a uniform asymptotic manner if we let ϵ approach zero. In this system the Tikhonov function F is given by

$$F = -(S_K - X_K)^2 - (S_A - X_A)^2 - (Z_A - Y_A)^2$$

which is negative definite over the whole phase space. We are therefore justified in determining the conditions for system 12 to have a stable limit cycle and expecting in this case that system 1 B, 3, 5, 7 will then also have a limit cycle.

Since the time constant of the $\dot{V}$ equation is much smaller than that of the $\dot{X}_P$ equation, we may approach this problem through the theory of discontinuous oscillations (Andronov et al., 1966), noting that the $\dot{V}$ term does not satisfy the condition of Tikhonov's theorem. To make the system autonomous (i.e. having a right-hand side independent of time), we assume that I_{ext} is a constant. According to this theory, the system 12 will have, for sufficiently large values of τ_{XP}, a unique stable limit cycle if its nullclines have the geometry of those shown in Fig. 12. In the phase plane of this system, the form of the Eqs. 12 determines everything but the shape of the nullcline $\dot{V} = 0$ near the equilibrium point (Plant and Kim, 1975). Therefore, there are only two conditions in addition to those already given which must be satisfied.

(*a*) The slope of the equation $X_P = G(V)$ obtained by solving $\dot{V} = 0$ must have a negative slope for all V except those in a single interval $V_1 < V < V_2$, in which $G'(V)$ must be positive.

(*b*) The curves $X_P = S_P(V)$ and $X_P = G(V)$ must have a unique intersection, and it must be in the region of positive $G'(V)$. The equation for $G(V)$ is given by

$$\begin{aligned} \dot{V} = 0: X_P \triangleq G(V) &= [1/g_P(V - V_K)][g_T(V_I - V) \\ &\quad - [g_K S_K^4(V) + g_A S_A(V) Z_A(V)](V - V_K) \\ &\quad + g_L(V_L - V) + I_{ep} + I_{ext}]. \end{aligned} \tag{13}$$

Noting that the signs of the derivative of the S and Z functions are uniformly positive and negative, respectively, we see that condition (*a*) is satisfied if there is a unique interval $V_1 \leq V \leq V_2$ such that

$$|Z_A' S_A| > (g_K/g_A)(S_K^4)' + S_A' Z_A + \frac{g_T(V_I - V_K) + g_L(V_K - V_L) + I_{ep} + I_{ext}}{g_A(V - V_K)^2} \tag{I}$$

and condition (*b*) is satisfied if

$$G(V^*) = S_P(V^*) \text{ for a unique } V^* \text{ such that } V_1 < V^* < V_2. \qquad \text{(II)}$$

Thus a sufficient condition for the system 12 to have a unique, stable limit cycle is that conditions I and II be satisfied and that τ_{XP} be large enough for the discontinuous approximation to be valid. If this is true, then for large τ_{XP} we may expect the full system 1 B, 3, 5, 7 to have a periodic, oscillatory solution. We note that the existence of such an oscillatory solution is not guaranteed, nor is it implied that conditions I and II are necessary for such a solution. This is particularly true for system 1 B, 3, 5, 7 because the time constants of parameters X_K, X_A, and Y_A vary among themselves by an order of magnitude (cf. Table III). Indeed, these parameters have in the past been referred to as being respectively "fast" and "slow," it is only with respect to X_P that they are all "relatively fast."

REFERENCES

ANDRONOV, A. A., A. A. VITT, and S. E. KHAIKEN. 1966. Theory of Oscillators. (Engl. Transl.). Addison-Wesley Publishing Co., Inc., Reading, Mass.

CARPENTER, D. O. 1973. Ionic Mechanisms and Models of Endogenous Discharge of *Aplysia* Neurones in Neurobiology of Invertebrates. J. Salanaki, editor. 35.

CONNOR, J. A., and C. F. STEVENS. 1971. Prediction of repetitive firing behavior from voltage clamp data on an isolated neurone soma. *J. Physiol.* **213**:31.

COOKE, I. M., G. LEBLANC, and L. TAUC. 1974. Sodium pump stoichiometry in *Aplysia* neurones from simultaneous current and tracer measurements. *Nature (Lond.).* **251**:254.

EATON, D. C. 1972. Potassium ion accumulation near a pace-making cell of *Aplysia*. *J. Physiol.* **224**:421.

FABER, D. S., and M. R. KLEE. 1972. Membrane characteristics of bursting pacemaker neurones in *Aplysia*. *Nat. New Biol.* **240**:29.

FITZHUGH, R. 1969. Mathematical models of excitation and propagation in nerve. *In* Biological Engineering. H.P. Schwann, editor. 1.

FRANKENHAEUSER, B., and A. L. HODGKIN. 1956. The after effects of impulses in the giant nerve fibers of *Loglio*. *J. Physiol.* **131**:341

FRAZIER, W. T., E. R. KANDEL, J. KUPFERMANN, R. WAZIRI, and R. E. COGGESHALL. 1967. Morphological and functional properties of identified neurons in the abdominal ganglion of *Aplysia californica*. *J. Neurophysiol.* **30**:1288.

GOLA, M. 1974. Neurones à Ondes-Salves des mollusques. *Pfluegers Arch. Eur. J. Physiol.* **352**:17.

HAMMING, R. W. 1973. Numerical Methods for Scientists and Engineers. McGraw-Hill Book Company, New York. 2nd edition.

HODGKIN, A. L., and A. F. HUXLEY. 1952. A quantitative description of membrane current and its application to conduction and excitation in nerve. *J. Physiol.* **117**:500.

JUNGE, D., and M. BRODWICH, 1970. Post-stimulus potassium conductance increase in *Aplysia* giant neurones. *Physiologist*. **13**:237.

JUNGE, D., and C. L. STEPHENS. 1973. Cyclic variation of potassium conductance in a burst generating neurone in *Aplysia*. *J. Physiol.* **235**:155.

LUX, H. D., and R. ECKERT. 1974. Inferred slow inward current in snail neurons. *Nature (Lond.).* **250**:574.

MATHIEU, P. A., and F. A. ROBERGE. 1971. Characteristics of pacemaker oscillations in *Aplysia* neurones. *Can. J. Physiol. Pharmacol.* **49**:787.

MOORE, J. W., and F. RAMON, 1974. On numerical integration of the Hodgkin and Huxley equations for a membrane action potential. *J. Theor. Biol.* **45**:249.

NARAHASHI, T., J. W. MOORE, and W. R. SCOTT. 1964. Tetrodotoxin blockage of sodium conductance increase in lobster giant axons. *J. Gen. Physiol.* **47**:965.

NOBLE, D. 1962. A modification of the Hodgkin-Huxley equations applicable to Purkinje fiber action and pacemaker potentials. *J. Physiol.* **160**:317.

PLANT, R. E., and M. KIM. 1975. On the mechanism underlying bursting in the *Aplysia* abdominal ganglion R15 cell. *Math. Biosci.* In press.

SASTRE, A. 1974. Analysis and Simulation of Pacemaker Neurons. Ph.D. Thesis. Cornell University, Ithaca, N.Y.

SMITH, T. G., J. L. BARKER, and H. GAINER. 1975. Requirements for bursting pacemaker potential activity in mollerscan neurons. *Nature (Lond.).* **253**:450.

STRUMWASSER, F. 1967. Types of information stored in single neutrons. *In* Invertebrate Nervous Systems. C.A.G. Wiersma, editor. 291.

STRUMWASSER, F. 1968. Membrane and intracellular mechanism governing endogenous activity in neurons. *In* Physiological and Biochemical Aspects of Nervous Integration. F. D. Carlson, editor. 329.

STRUMWASSER, F. 1973. Neural and humoral factors in temporal organization of behavior. *Physiologist.* **16**:9.

TIKHONOV, A. N. 1950. On systems of equations containing parameters. (In Russian). *Mater. Sb.* **27**:147.

WACHTEL, H., and W. A. WILSON. 1973. Voltage clamp analysis of rhythmic slow generation in bursting neurones. *In* Neurobiology of Invertebrates. J. Salanki, editor. 59.

WILSON, W. A., and H. Wachtel. 1974. Negative resistance characteristic essential for the maintenance of slow oscillations in bursting neurons. *Science (Wash. D.C.).* **186**:932.

WINFREE, A. 1970. The temporal morphology of a biological clock. *In* Symposia on Math. Biol. 2nd and 3rd, 109.